Dalton Transactions

Accepted Manuscript

This article can be cited before page numbers have been issued, to do this please use: P. Gamez, J. Grau, C. Renau, A. B. Caballero, A. Caubet, M. Pockaj and J. Loreznco, *Dalton Trans.*, 2018, DOI: 10.1039/C7DT04604A.

ROYAL SOCIETY OF CHEMISTRY

rsc.li/dalton

View Article Online
DOI: 10.1039/C7DT04604A

Dalton Transactions

PAPER

Evaluation of the metal-dependent cytotoxic behaviour of coordination compounds

Received 00th January 2018,
Accepted 00th January 2018

DOI: 10.1039/x0xx00000x

www.rsc.org/

Jordi Grau,[a] Cristina Renau,[a] Ana B. Caballero,[a] Amparo Caubet,*[a] Marta Pockaj,[b] Julia Lorenzo[c] and Patrick Gamez*[ade]

The **[Cu(L)Cl$_2$]$_2$** and **[Pt(L)Cl$_2$]** complexes were prepared from the simple Schiff-base ligand (*E*)-phenyl-*N*-((pyridin-2-yl)methylene)methanamine (**L**) and respectively, $CuCl_2$ and *cis*-[$PtCl_2(DMSO)_2$]. DNA-interaction studies revealed that the copper complex most likely acts as a DNA cleaver whereas the platinum complex binds to the double helix. Remarkably, cell-viability experiments with HeLa, MCF7 and PC3 cells showed that **[Cu(L)Cl$_2$]$_2$** is an efficient cytotoxic agent whereas **[Pt(L)Cl$_2$]** is not toxic, illustrating the crucial role played by the nature of the metal ion on the corresponding biological activity.

Introduction

Since the fortuitous discovery of the anticancer properties of *cis*-diamminedichloridoplatinum(II), cisplatin, by Rosenberg and co-workers in the 1960s,[1, 2] there has been growing interest in the design of platinum-based drugs,[3, 4] and more generally of metal complexes as potential chemotherapeutic agents.[5]

Coordination compounds offer high versatility for drug design; indeed, besides the nature of the metal and its oxidation state, various geometries and coordination numbers may be adopted by metal ions, which allow to fine-tune their chemical reactivity through the adjustment of kinetic (rates of ligand exchange) and/or thermodynamic (metal–ligand bond strengths, redox potentials, etc.) parameters.[6] The ligands may also be involved in the observed biological activity of the complexes, through (i) their participation in the outer-sphere recognition of the target site,[7] (ii) the (cytotoxic) activity of any released ligands[8] or (iii) ligand-centred redox processes.[9]

Apart from platinum, other transition-metal ions are used to develop potential anticancer metallodrugs.[10, 11] In that context, copper represents a good alternative as it is an essential trace element present in the human body (it is therefore biocompatible). Moreover, copper is naturally more abundant than platinum, and is thus far cheaper than the precious metal. Actually, since the initial work of Sigman and co-workers in the 1970s,[12, 13] the scientific community has shown increasing interest in copper complexes.[14] For instance, some mixed-chelate copper complexes of the Casiopeínas® family have entered clinical trials.[15]

In the present study, a very simple, readily available Schiff-base ligand, namely (*E*)-phenyl-*N*-((pyridin-2-yl)methylene)methanamine[16, 17] (**L**; Figure 1), has been used to generate two different coordination compounds from the metal chloride salts *cis*-[$PtCl_2(DMSO)_2$] and $CuCl_2$. Comparison of the DNA-interacting and cytotoxic behaviours of the complexes obtained, *i.e.* **[Pt(L)Cl$_2$]** and **[Cu(L)Cl$_2$]$_2$**, reveals that the nature of the metal ion has a drastic effect on the biological properties of the corresponding "**[M(L)Cl$_2$]**" compound.

Experimental

Materials and methods

Reagents and solvents were obtained from Sigma-Aldrich or Fisher Scientific and used as received. pBR322 plasmid DNA and calf-thymus DNA (ct-DNA) were purchased from Sigma-Aldrich.

Nuclear magnetic resonance (^{1}H and ^{13}C{^{1}H}) spectra were recorded at room temperature on a Varian Unity 400 MHz spectrometer. Proton chemical shifts are expressed in parts per million (ppm, δ scale) and are referenced to residual solvent peaks. Infrared (IR) spectra (KBr pellets) were recorded with a Nicolet-5700 FT-IR (in the range 4000–400 cm^{-1}), and data are represented as the frequency of absorption in cm^{-1}.

[a] Department of Inorganic and Organic Chemistry, University of Barcelona, Martí i Franquès 1-11, 08028 Barcelona, Spain. E-mail: patrick.gamez@qi.ub.es
[b] Faculty of Chemistry and Chemical Technology, University of Ljubljana, Večna pot 113, SI-1000 Ljubljana, Slovenia.
[c] Institut de Biotecnologia i de Biomedicina and Departament de Bioquímica i de Biologia Molecular, Universitat Autònoma de Barcelona, Bellaterra, Barcelona, Spain.
[d] Catalan Institution for Research and Advanced Studies (ICREA), Passeig Lluís Companys 23, 08010 Barcelona, Spain.
[e] Institute of Nanoscience and Nanotechnology (IN2UB), Universitat de Barcelona

† Footnotes relating to the title and/or authors should appear here.

Electronic Supplementary Information (ESI) available: Crystal data and structure refinement for **[Cu(L)Cl$_2$]$_2$** (Table S1), representation of the X-ray structure of **[Cu(L)Cl$_2$]$_2$** (Figure S1) and selected coordination bond distances and angles for **[Cu(L)Cl$_2$]$_2$** (Table S2). CCDC 1585826. For ESI and crystallographic data in CIF or another electronic format, see DOI: 10.1039/x0xx00000x

View Article Online
DOI: 10.1039/C7DT04604A

Elemental analyses were carried out by the Serveis Científic i Tecnològics de la Universitat de Barcelona. UV-Vis experiments were performed with a Varian Cary-100 spectrophotometer, and fluorescence measurements were achieved using a HORIBA Jobin–Yvon iHR320 spectrofluorimeter at room temperature. The photomultiplier detector voltage was set at 950 V, and the instrument excitation and emission slits were both set at 5 nm. The concentrations of DNA and complexes used for the UV-vis and fluorescence studies are described in the section Results and Discussion.

Preparation of the ligand L and the complexes [[Pt(L)Cl$_2$] and [Cu(L)Cl$_2$]$_2$.

Ligand: The ligand (*E*)-phenyl-*N*-((pyridin-2-yl)methylene)methanamine[16] (Scheme 1, **L**) was prepared by

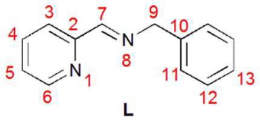

L

condensation of pyridine-2-carbaldehyde and benzylamine. **L** was obtained as an oil, with a yield of 70%.

^{1}H NMR (400 MHz, $CDCl_3$): δ = 8.62 (d, 1H, H6), 8.47 (s, 1H, H7), 8.05 (d, 1H, H3), 7.71 (t, 1H, H4), 7.27 (m, 2H, H11 and H12), 7.23 (t, 1H, H5), 7.20 (t, 1H, H13), 4.86 (s, 2H, H9). ^{13}C{^{1}H}-NMR (101 MHz, $CDCl_3$, ppm): δ = 164.3 (C7), 156.0 (C2), 150.8 (C6), 140.1 (C10), 138.1 (C4), 130.0 (C12), 129.7 (C11), 128.7 (C13), 126.3 (C5), 122.8 (C3), 66.4 (C9). IR (KBr, cm^{-1}): 3383 (ν(NH)), 3100-3000 (ν(C_{sp2}H)), 1643 (ν(C=N)), 1188 (ν(C-N)).

[Pt(L)Cl$_2$]: a methanolic solution of *cis*-[$PtCl_2(DMSO)_2$] (0.211 g; 0.5 mmol; 20 mL) was refluxed until dissolution of the platinum precursor. After filtration, a methanolic solution of ligand **L** (0.106 g; 0.5 mmol; 3 mL) was added and the resulting reaction mixture was stirred at room temperature for 30 minutes. Subsequently, the orange precipitate was isolated by filtration and washed with methanol. After drying in air, 0.091 g of the platinum(II) complex

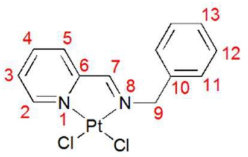

was obtained (Yield = 39%). Elemental analysis calcd. for $C_{13}H_{12}Cl_2N_2Pt$ (%): C 33.78, H 2.62, N 6.06; found: C 33.62, H 2.63, N 6.06. ^{1}H NMR (400 MHz, [D_6]DMSO): δ = 9.37 (d, 1H, H2), 9.30 (s, 1H, H7), 8.37 (t, 1H, H4), 8.16 (d, 1H, H5), 7.91 (t, 1H, H3), 7.53 (d, 1H, H11), 7.40 (t, 1H, H12), 7.35 (t, 1H, H13), 5.32 (s, 2H, H9). ^{13}C{^{1}H}-NMR (101 MHz, [D_6]DMSO, ppm): δ = 171.9 (C7), 156.9 (C6), 148.8 (C2), 140.5 (C4), 138.2 (C10), 136.0 (C3), 129.2 (C5), 128.8 (C11), 128.4 (C12), 128.0 (C13), 60.9 (C9). IR (KBr, cm^{-1}): 3100-3000 (ν(C_{sp2}H)), 1622 (ν(C=N)), 522 and 448 (ν(Pt-N)).

[Cu(L)Cl$_2$]$_2$: An ethanolic solution of ligand **L** (39.3 mg, 0.2 mmol; 5 mL) was added to an ethanolic solution of $CuCl_2 \cdot 2H_2O$ (34.0 mg, 0.2 mmol; 15 mL). The resulting green solution was left unperturbed for the slow evaporation of the solvent. Green single crystals, suitable for X-ray diffraction measurements (see Supporting Information for X-ray data), were obtained with a yield of 51% (based on copper). Elemental analysis calcd. for $C_{26}H_{24}Cl_4N_4Cu_2$ (%): C 47.21, H 3.66, N 8.47; found: C 47.38, H 3.89, N 8.58. IR (KBr, cm^{-1}): 3439 (ν(OH) + ν(NH)), 3065 (ν(C_{sp2}H)), 1608 (ν(C=N)), 1062 (ν(C-N)).

Gel Electrophoresis.

[Cu(L)Cl$_2$]$_2$: a stock solution of the complex was prepared in 1 mM sodium cacodylate–20 mM NaCl buffer (pH = 7.2). pBR322 plasmid DNA aliquots (0.01 mg mL^{-1}, 15 μM referred to base pairs) in 1 mM cacodylate–20 mM NaCl buffer were incubated with **[Cu(L)Cl$_2$]$_2$** for 1 h at 37 °C. Subsequently, ascorbic acid (1 mM cacodylate–20 mM NaCl buffer) was added (in the case of the experiments without ascorbic acid, this step was not done), and the resulting mixture was incubated at 37 °C for an additional hour. Next, the reaction samples were quenched with 4 μL of a solution containing 30% (v/v) glycerol and 0.25% (w/v) xylene cyanol, and then electrophoretized on agarose gel (1% in TAE buffer, Tris-acetate–EDTA) for 2 h at 1.5 V cm^{-1}. The electrophoresis was carried out using a BIORAD horizontal tank connected to a CONSORT EV231 variable potential power supply. Samples of free DNA and DNA in the presence of ascorbic acid were used as controls. Afterwards, the DNA was stained with SYBR® safe and the gel was photographed with a BIORAD Gel Doc™ EZ Imager.

[Pt(L)Cl$_2$]: Solutions containing 10-100 uM of the complex, 1 % DMSO and 15 μM_{bp} pBR322 plasmid DNA were incubated for 24 h at 37 °C. Next, the reaction samples were quenched with 4 μL of a solution containing 30% (v/v) glycerol and 0.25% (w/v) xylene cyanol, and then electrophoretized on agarose gel (1% in TBE buffer 1X, Tris-Borate–EDTA) for 1 h at 6.25 V cm^{-1}.

X-ray crystallography. Single-crystal X-ray diffraction.

A single crystal of **[Cu(L)Cl$_2$]$_2$** in silicon grease was mounted on the tip of a glass fibre and transferred to the goniometer head, under a cryostream of nitrogen. Data were collected on a SuperNova diffractometer equipped with an Atlas detector, using CrysAlis PRO software, and monochromated Mo Kα radiation (0.71073 Å) at 150 K.[18] The initial structural model containing the coordination molecule was obtained using the Superflip structure solution program.[19] Full-matrix least-squares refinement on F^2 with anisotropic displacement parameters for all nonhydrogen atoms was carried out using SHELXL2017.[20] All H atoms were initially located in difference Fourier maps and were further treated as riding on their parent atoms with C(aromatic)–H = 0.95 Å and C(methylene)–H = 0.99 Å. Details on crystal data, data collection and structure refinement are given in the Supporting Information.

These data can be obtained free of charge from the Cambridge Crystallographic Data Center via https://summary.ccdc.cam.ac.uk/structure-summary-form.

View Article Online
DOI: 10.1039/C7DT04604A

Cell-line culture and cell viability assays

The cancer cells (HeLa, MCF7 and PC3 cell lines) were cultured in Minimum Essential Medium (MEM) alpha medium supplemented with 10% (v/v) heat inactivated fetal bovine serum (FBS) in a highly humidified atmosphere of 95% air with 5% $C0_2$ at 37 °C.

Cytotoxicity was determined using PrestoBlue cell viability assay (ThermoFisher). The cells were seeded in a 96-well microtiter plate at a concentration of 1×10^4 cells per well and incubated overnight in an atmosphere containing 5% CO_2 at 37 °C. The cells were exposed to the positive drug control cisplatin, to the free ligand **L**, and to complexes **[Pt(L)Cl$_2$]$_2$** and **[Cu(L)Cl$_2$]$_2$**. The microtiter plate was incubated for 24 h or 72 h, and 20 µL of PrestoBlue were subsequently added. The plates were incubated for 2 additional hours, and the fluorescence was measured exciting at 531 nm and 570 nm, using a Victor3 V multiwell plate reader (Perkin Elmer). The cytotoxicity of each sample was expressed as the IC_{50} value, which is the concentration of the complex that caused 50% inhibition of cell growth. All the samples were assayed in triplicate.

The induction of apoptosis *in vitro* by the different complexes was determined with HeLa cells by a flow cytometric assay with Annexin V-FITC, using the Annexin V-FITC apoptosis detection kit from Roche. Exponentially growing HeLa cells in 6-well plates (4×10^5 cells per well) were exposed to concentrations equal to the IC_{50} values at 24 h of the complexes, or cisplatin as a reference. The cells were collected, washed with PBS, and resuspended in 100 µL of binding buffer. 2 µL of Annexin V-fluorescein isothiocyanate (FITC) and 2 µL of propidium iodide (PI) were added to the samples for 15 min at room temperature in the dark. The number of apoptotic cells was analysed by flow cytometry (FacsCalibur, Becton Dickinson).

Results and discussion

The ligand (*E*)-phenyl-*N*-((pyridin-2-yl)methylene)methanamine (**L**) was obtained in good yield by simple condensation reaction between benzylamine and 2-pyridinecarboxaldehyde, in ethanol under reflux. The complexes were prepared by mixing equivalent amounts of ligand **L** and the respective metal-chloride precursor in an alcoholic solvent (see Experimental Section). **[Pt(L)Cl$_2$]** was obtained in methanol with a yield of 39% while **[Cu(L)Cl$_2$]$_2$** was isolated from an ethanolic solution with a yield of 51%. Single crystals of the copper complex were obtained, whose X-ray diffraction analysis confirmed the structure previously described in the literature (Figure S1).[21] Crystallographic data for **[Cu(L)Cl$_2$]$_2$** are summarized in Table S1, and selected coordination bond lengths and angles are listed in Table S2. It is important to notice that the two metal complexes display similar coordination environments, which is illustrated in Figure 1. In both cases, a square plane is present, formed through the *cis*-coordination of a chelating **L** ligand and two chlorides to the metal center. It can be stressed that, in the solid state, the copper complex is a chlorido-bridged dimer (see Figure S1). However, since one of the Cl anions is semi-coordinated to the Cu ion (Cu–Cl distance superior to 2.6 Å; see Table S2), it can be expected that the bis-µ-Cl bridge is broken in solution,[22] generating a mononuclear species.

The interaction of the two complexes with DNA was subsequently examined using different techniques.

UV-vis studies. The interaction of **[Cu(L)Cl$_2$]$_2$** and **[Pt(L)Cl$_2$]** with DNA was first investigated by UV-vis spectrophotometric titration. Addition of increasing amounts of ct-DNA (from 0 to 100 µM, in base pairs) to a 25 µM solution of **[Cu(L)Cl$_2$]$_2$** resulted in clear hypochromicity but no absorption shift was observed (Figure 2). These features suggest that **[Cu(L)Cl$_2$]$_2$** interacts outside the minor groove of DNA.[23] The corresponding K_b value of (1.4 ± 0.2) 10^5 M^{-1} was determined by plotting [DNA]/(ε_f–ε_a) *versus* [DNA], ε_f being the extinction coefficient of the free complex in solution (A_{obs}/[complex]) and ε_a the extinction coefficient of the DNA-bound complex (insert in Figure 2).

For **[Pt(L)Cl$_2$]**, hypochromicity with a slight red shift (Δλ = 2 nm) of the absorption is observed (Figure 3). The small bathochromic effect associated with the decrease of the absorption intensity can be ascribed to intercalation, but outside binding cannot be excluded (indeed, strong intercalation is characterized by a large red shift, of more than 10 nm).[24] These data indicate that **[Pt(L)Cl$_2$]** most likely interacts with DNA *via* different binding modes. The determined K_b value of (7.2 ± 0.1) × 10^6 M^{-1} illustrates a stronger DNA interaction of **[Pt(L)Cl$_2$]**, compared with that of **[Cu(L)Cl$_2$]$_2$**.

Fluorescence studies. The ability of **[Cu(L)Cl$_2$]$_2$** to displace the DNA-intercalator ethidium bromide (EB) was evaluated using fluorescence spectroscopy. Increasing amounts of the copper compound (0–100 µM) have been added to a solution of the fluorescent EB-DNA complex (constant concentrations of EB and ct-DNA of 25.36 mM and 25 µM, respectively). A moderate decrease in emission intensity is achieved (Figure 4), which also indicates that **[Cu(L)Cl$_2$]$_2$** is not acting as an intercalator (see UV-vis data). It can be pointed out here that the poor displacement of EB observed may indeed be explained by electrostatic interactions or groove binding; such interactions can be sufficient to modify the conformation of the DNA double helix, resulting in the release of EB.[25, 26] The corresponding Stern-Volmer quenching constant (K_{SV}), determined by plotting I_0/I versus [complex] (I_0 and I being the emission intensities in the absence and the presence of the complex, respectively),[27] is (1.9 ± 0.1) × 10^3 M^{-1}. This value illustrates poor intercalating properties for the copper compound, as already inferred from the UV-vis studies (see above); most likely, **[Cu(L)Cl$_2$]$_2$** acts as a groove binder.

In the case of the platinum complex, a non-linear I_0/I *vs.* [complex] plot is obtained (Figure 5). As for the UV-vis study (see above), the fluorescence data also indicate that **[Pt(L)Cl$_2$]** interacts through various modes of binding with the double helix. The Stern-Volmer constant was determined for the initial points of the plot, namely for complex concentrations of 0, 5, 10 and 15 µM (insert of Figure 5). The obtained K_{SV} of (7.5 ±

View Article Online
DOI: 10.1039/C7DT04604A

0.5) × 10^3 M^{-1} suggests that the platinum compound has some DNA-intercalating behaviour at low [complex]. For [complex] > 15 μM, no release of EB is observed, which may be explained by another mode of interaction, for instance groove binding (as corroborated by the UV-vis data; see above).

Gel electrophoresis. The interaction of **$[Cu(L)Cl_2]_2$** with DNA was directly observed with agarose gel electrophoresis. Electrophoretic mobility measurements of pBR322 plasmid DNA were therefore carried out using increasing amounts of the copper complex (5–100 μM). Ascorbic acid was used as reducing agent, which mimics the reducing environment found inside cells. The resulting generation of copper(I) species is thus expected to mediate the formation of reactive oxygen species that will cleave DNA. The consequent agarose gel is depicted in Figure 6a. As expected, pure plasmid DNA ([DNA] = 15 μM in base pairs) gives two bands (lane 1), the most intense one corresponding to supercoiled DNA (form I), while the second one is ascribed to the circular nicked form (form II). In the absence of ascorbic acid (lanes 2–8), **$[Cu(L)Cl_2]_2$** does not affect the structure of the biomolecule. Similarly, the well-known DNA cleaver $[Cu(phen)_2]^{2+}$ (which is the copper-based chemical nuclease of reference)[28] is not active with no added reducing agent (lane 9; [complex] = 40 μM). In contrast, when ascorbic acid is added to $[Cu(phen)_2]^{2+}$, a complete degradation of DNA is observed (lane 10). It can be noticed that in the sole presence of the reducing agent, *i.e.* without the copper compound, the DNA is not altered (lane 11). For **$[Cu(L)Cl_2]_2$**, as for the copper-phenanthroline complex, the presence of reducing agent gives rise to DNA cleavage (lanes 12–19). Already at a complex concentration of 5 μM, an increase in form II is noticed (form II is obtained when one of the two strands are cut apart), which is associated to a decrease in form I (lane 12). At a concentration of 20 μM, form I has completely disappeared and the linear form, *i.e.* form III resulting from the breakage of both strands, is observed (lane 15). From a complex concentration of 40 μM, total degradation of DNA is achieved (lanes 16–19). Hence, **$[Cu(L)Cl_2]_2$** appears to be at least as active as the reference compound $[Cu(phen)_2]^{2+}$ (see lanes 10 and 16). Thus, although **$[Cu(L)Cl_2]_2$** is not strongly interacting with DNA (see UV-vis and fluorescence data above), most likely it induces the formation of radical species (such as Sigman's reagent, *i.e.* $[Cu(phen)_2]^{2+}$)[29] that are really harmful to the biomolecule.

The gel electrophoresis results for **$[Pt(L)Cl_2]$** are shown in Figure 6b. Incubation of DNA with 0.5 equivalents of cisplatin affects the electrophoretic mobility of both form I and form II; cisplatin-mediated unwinding of form I causes a diminution of its mobility, whereas the unwinding of form II increases its mobility because of a shortening effect on the DNA contour length (see lanes 1 and 2).[30, 31] These effects become even more pronounced when the concentration of cisplatin is increased, up to the point that the two bands coalesce; in fact, a single broad band is observed when 1.0 equivalent is used (lane 3). 0.67 and 1.67 equivalents of **$[Pt(L)Cl_2]$** appear to induce the unwinding of form I, converting it into form II (lanes 4 and 5). This may be explained by single-strand cleavage of the plasmid upon platinum binding. A higher complex concentration, namely 50 μM (3.33 equivalents), shows a different behaviour (lane 6); indeed, a combination between a cisplatin-like effect and single-stand break is observed, suggesting that the binding of the complex eventually leads to the cleavage of the biomolecule. Actually, at a concentration of 100 μM (6.67 equivalents), complete relaxation of supercoiled DNA (form I) is observed, and the sole presence of form II is detected. tend

Cytotoxicity assays. Cytotoxicity studies were carried out for both compounds with HeLa (cervical carcinoma),[32] MCF7 (breast adenocarcinoma) and PC3 (prostatic small cell carcinoma) cells. The aim was to illustrate that copper compounds may offer an alternative to platinum drugs. The cytotoxic behaviour of both complexes was thus investigated and compared with that of the free ligand **L**, copper(II) chloride and cisplatin. The IC_{50} values obtained after 24 and 72 hours of incubation with the three different cell lines are listed in Table 1.

Table 1 IC_{50} values (μM) for the two complexes, the free ligand **L**, copper(II) chloride and cisplatin against HeLa, MCF7 and PC3 cells, after 24 and 72 h incubation.

	HeLa	
Complex	24 h	72 h
$[Pt(L)Cl_2]$	> 100	73.9 ± 4.1
$[Cu(L)Cl_2]_2$	**8.5 ± 1.3**	**7.7 ± 1.4**
Ligand **L**	n.a.[a]	n.a.[a]
$CuCl_2$	n.a.[a]	> 200
cisplatin	40.3 ± 3.7	14.7 ± 2.6
	MCF7	
$[Pt(L)Cl_2]$	> 100	45.5 ± 6.1
$[Cu(L)Cl_2]_2$	13.6 ± 1.2	**5.1 ± 1.1**
Ligand **L**	n.a.[a]	n.a.[a]
$CuCl_2$	n.a.[a]	> 200
cisplatin	38.3 ± 3.2	5.6 ± 0.4
	PC3	
$[Pt(L)Cl_2]$	> 100	78.8 ± 8.8
$[Cu(L)Cl_2]_2$	17.2 ± 2.9	**9.7 ± 1.1**
Ligand **L**	n.a.[a]	n.a.[a]
$CuCl_2$	n.a.[a]	> 200
cisplatin	49.8 ± 5.4	7.4 ± 0.9

[a] n.a. stands for ´not active´ and indicates that IC_{50} values could not be obtained (due to non-cytotoxicity).

The copper complex **$[Cu(L)Cl_2]_2$** exhibits very good cytotoxic properties; after 24 h incubation with HeLa cells, an IC_{50} value of 8.5 ± 1.3 μM is reached (Table 1). In contrast, the platinum compound **$[Pt(L)Cl_2]$** is not active. After 72 hours of incubation, **$[Cu(L)Cl_2]_2$** is 10 times more active than **$[Pt(L)Cl_2]$**; *i.e.* 7.7 ± 1.4 *versus* 73.9 ± 4.1 μM, respectively. The free ligand **L** is not cytotoxic so as copper(II) chloride. Cisplatin shows some moderate activity against this line, albeit superior to that observed for **$[Pt(L)Cl_2]$**. With MCF7 cells, the same tendency is observed, the copper compound being 9 times more active than the platinum one (*i.e.* 5.1 ± 1.1 *versus* 45.5 ± 6.1 μM). The

View Article Online
DOI: 10.1039/C7DT04604A

higher toxicity of **$[Cu(L)Cl_2]_2$** is further confirmed using PC3 cells; after 72 h incubation, its IC_{50} value for this cell line is 9.7 ± 1.1 while it is 78.8 ± 8.8 for **$[Pt(L)Cl_2]$**. The cytotoxic activities of **$[Cu(L)Cl_2]_2$** against MCF7 and PC3 cells are comparable to that of cisplatin.

In all cases, **$[Cu(L)Cl_2]_2$** is clearly the most active compound, which illustrates the crucial role played by the metal ion. Indeed, **$[Cu(L)Cl_2]_2$** and **$[Pt(L)Cl_2]$** have similar coordination environments built up from the same ligands, namely chloride anions and the simple bidentate ligand (*E*)-phenyl-N-((pyridin-2-yl)methylene)methanamine (ligand **L**). Remarkably, **L** is non-cytotoxic and **$[Pt(L)Cl_2]$** is poorly cytotoxic, whereas **$[Cu(L)Cl_2]_2$** displays an interesting behaviour (Table 1).

In summary, although **$[Pt(L)Cl_2]$** appears to better interact with DNA than **$[Cu(L)Cl_2]_2$** (see above), it exhibits significantly lower cytotoxicities than the copper compound. Clearly, the formation of reactive oxygen species (ROS) mediated by the redox-active copper complex is crucial regarding cell toxicity.

Subsequently, the ability of **$[Cu(L)Cl_2]_2$** to induce apoptosis was examined and compared with that of cisplatin, using HeLa cells. The experiments were carried out using an incubation time of 24 hours, and complex concentrations corresponding to the IC_{50} value for each compound at this incubation period (see Table 1; HeLa cells). The results obtained are shown in Table 2.

Table 2 Percentage of HeLa cells in each state after 24 hours of incubation, in the absence (control) and presence of IC_{50} concentrations (see Table 1; 24 h) of **$[Cu(L)Cl_2]_2$** and cisplatin.

Treatment (IC_{50}, 24 h)	% vital cells (**R1**)	% apoptotic cells (**R2**)	% late apoptosis or dead cells (**R3**)	% damaged cells (**R4**)
control	90.5	4.7	3.3	1.6
$[Cu(\mathbf{L})Cl_2]_2$	68.9	16.6	13.1	1.3
cisplatin	62.2	23.9	13.4	0.5

Interestingly, the copper complex induces apoptosis of HeLa cells, albeit in a slightly less efficient manner than cisplatin (17% versus 24%; Table 2). Thus, it appears that **$[Cu(L)Cl_2]_2$** causes apoptotic cell death through a mechanism of action, *i.e.* production of ROS, which is different to that of the well-known platinum compound.

Conclusions

Since the first report of Sigman's reagent in the late 1970s,[12, 13] copper complexes have increasingly been investigated as a potential alternative to platinum drugs.[28] It is well known that most Pt complexes target DNA, and it is believed that it is also the case for a number of Cu coordination compounds.[29] However, one should also bear in mind that copper is redox active, and can therefore be involved in the generation of ROS, which are highly harmful species that can affect/damage DNA, so as any other cellular components. In other words, a cytotoxic behaviour observed for a copper complex is not necessarily due to its binding to DNA (*i.e.* cisplatin-like mode of action) but can result from oxidative stress (Sigman-like mode of action).

In the present study, a copper and a platinum complexes have been prepared from the same organic ligand, namely (*E*)-phenyl-*N*-((pyridin-2-yl)methylene)methanamine, and inorganic counter-ions, *viz.* chloride anions. The DNA-interacting properties of the two related compounds (differing by their metal centre) were examined, and their cytotoxicity behaviour was compared using HeLa, MCF7 and PC3 cells.

The results achieved are very instructive; indeed, the two compounds appear to affect DNA, but with different mechanisms of action. While the Cu complex clearly induces DNA cleavage, acting like Sigman's reagent, the platinum complex exhibits a behaviour that is analogous to that of cisplatin. Nevertheless, the platinum complex is poorly cytotoxic (*i.e.*, it is not active after 24 h incubation), whereas the copper complex is significantly cytotoxic (IC_{50} values in the range 8.5-17.2 µM after 24 h incubation). Remarkably, the free ligand nor copper(II) chloride show cytotoxicity, therefore illustrating the crucial effect of the association copper-ligand on the biological activity. Moreover, the role played by the nature of the coordinated metal ion is key as the same ligand leads to metal complexes with drastically distinct behaviours.

As recently mentioned in a review paper,[29] more systematic studies are needed to appraise the potential of copper complexes as anti-cancer agents to substitute platinum drugs; herein, it has been shown that a ligand generating a non-active Pt complex produces an active Cu complex, which induces cell apoptosis. These results hence indicate that metal screening with a ligand is important as it may allow to identify coordination compounds with interesting properties.

Acknowledgements

Financial support from the Spanish Ministerio de Economía y Competitividad (projects CTQ2015-70371-REDT, CTQ2014-55293-P and CTQ2017-88446-R) is acknowledged. PG acknowledges the Institució Catalana de Recerca i Estudis Avançats (ICREA).

References

1. B. Rosenberg, L. van Camp and T. Krigas, *Nature*, 1965, **205**, 698-699.
2. B. Rosenberg, L. van Camp, E. B. Grimley and A. J. Thomson, *J. Biol. Chem.*, 1967, **242**, 1347-1352.
3. J. Reedijk, *Eur. J. Inorg. Chem.*, 2009, 1303-1312.
4. M. J. Hannon, *Pure Appl. Chem.*, 2007, **79**, 2243-2261.
5. K. B. Garbutcheon-Singh, M. P. Grant, B. W. Harper, A. M. Krause-Heuer, M. Manohar, N. Orkey and J. R. Aldrich-Wright, *Curr. Top. Med. Chem.*, 2011, **11**, 521-542.
6. I. Romero-Canelon and P. J. Sadler, *Inorg. Chem.*, 2013, **52**, 12276-12291.
7. B. J. Pages, D. L. Ang, E. P. Wright and J. R. Aldrich-Wright, *Dalton Trans.*, 2015, **44**, 3505-3526.
8. I. Ott and R. Gust, *Arch. Pharm.*, 2007, **340**, 117-126.

View Article Online
DOI: 10.1039/C7DT04604A
ARTICLE
Dalton Transactions

9. S. J. Dougan, A. Habtemariam, S. E. McHale, S. Parsons and P. J. Sadler, *Proc. Natl. Acad. Sci. U. S. A.*, 2008, **105**, 11628-11633.
10. M. Zaki, F. Arjmand and S. Tabassum, *Inorg. Chim. Acta*, 2016, **444**, 1-22.
11. J.-A. Cuello-Garibo, C. C. James, M. A. Siegler and S. Bonnet, *Chem. Sq.*, 2017, **1**, 2.
12. D. S. Sigman, D. R. Graham, V. Daurora and A. M. Stern, *J. Biol. Chem.*, 1979, **254**, 2269-2272.
13. V. Daurora, A. M. Stern and D. S. Sigman, *Biochem. Biophys. Res. Commun.*, 1978, **80**, 1025-1032.
14. C. Santini, M. Pellei, V. Gandin, M. Porchia, F. Tisato and C. Marzano, *Chem. Rev.*, 2014, **114**, 815-862.
15. L. Becco, J. C. Garcia-Ramos, L. R. Azuara, D. Gambino and B. Garat, *Biol. Trace Elem. Res.*, 2014, **161**, 210-215.
16. R. M. Ceder, G. Muller, M. Ordinas and J. I. Ordinas, *Dalton Trans.*, 2007, 83-90.
17. R. Garcia-Rodriguez and D. Miguel, *Dalton Trans.*, 2006, 1218-1225.
18. , Agilent Technologies Ltd, Yarnton, Oxfordshire, England, Editon edn., 2014.
19. L. Palatinus and G. Chapuis, *J. Appl. Crystallogr.*, 2007, **40**, 786-790.
20. G. M. Sheldrick, *Acta Crystallogr. Sect. C-Struct. Chem.*, 2015, **71**, 3-8.
21. N. Sengottuvelan, H. W. Lee, H. J. Seo, J. S. Choi, S. K. Kang and Y. I. Kim, *Bull. Korean Chem. Soc.*, 2008, **29**, 1711-1716.
22. K. Das, A. Datta, C. Sinha, J. H. Huang, E. Garribba, C. S. Hsiao and C. L. Hsu, *ChemistryOpen*, 2012, **1**, 80-89.
23. J. Chai, J. Y. Wang, Q. F. Xu, F. Hao and R. T. Liu, *Mol. BioSyst.*, 2012, **8**, 1902-1907.
24. L. Hassani, Z. Fazeli, E. Safaei, H. Rastegar and M. Akbari, *J. Biol. Phys.*, 2014, **40**, 275-283.
25. J. B. Lepecq and C. Paoletti, *J. Mol. Biol.*, 1967, **27**, 87-106.
26. F. J. Meyer-Almes and D. Porschke, *Biochemistry*, 1993, **32**, 4246-4253.
27. R. F. Brissos, E. Torrents, F. M. D. Mello, W. C. Pires, E. D. P. Silveira-Lacerda, A. B. Caballero, A. Caubet, C. Massera, O. Roubeau, S. J. Teate and P. Gamez, *Metallomics*, 2014, **6**, 1853-1868.
28. R. F. Brissos, A. Caubet and P. Gamez, *Eur. J. Inorg. Chem.*, 2015, 2633-2645.
29. T. J. P. McGivern, S. Afsharpour and C. J. Marmion, *Inorg. Chim. Acta*, 2017, **472**, 12-39.
30. G. L. Cohen, W. R. Bauer, J. K. Barton and S. J. Lippard, *Science*, 1979, **203**, 1014-1016.
31. S. E. Sherman and S. J. Lippard, *Chem. Rev.*, 1987, **87**, 1153-1181.
32. W. Small, M. A. Bacon, A. Bajaj, L. T. Chuang, B. J. Fisher, M. M. Harkenrider, A. Jhingran, H. C. Kitchener, L. R. Mileshkin, A. N. Viswanathan and D. K. Gaffney, *Cancer*, 2017, **123**, 2404-2412.

View Article Online
DOI: 10.1039/C7DT04604A
Dalton Transactions ARTICLE

Figure 1. Schematic illustration of the coordination environment of the metal centres, showing the formation of a square plane from a cis N2 ligand (**L**) and to chlorides.

Figure 2. Absorption spectra of $\mathbf{[Cu(L)Cl_2]_2}$ upon addition of ct-DNA. Complex concentration = 25 μM; [DNA] = 0–100 μM (DNA concentration determined at λ = 260 nm, with ε = 6600 M^{-1} cm^{-1}). The MLCT band at λ = 288 nm was used to determine K_b (insert). The blue arrows show the decrease in absorption intensity with the increase of [ct-DNA].

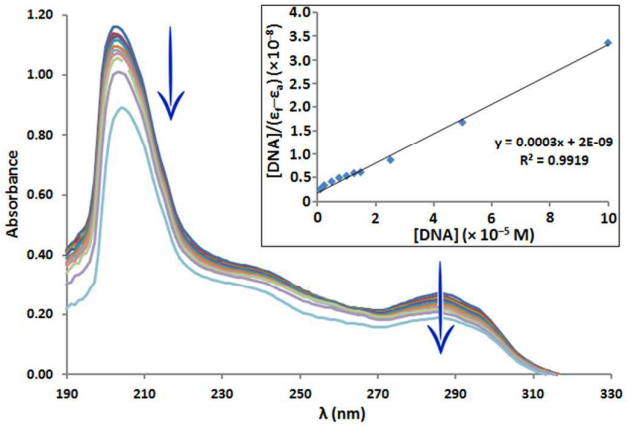

Figure 3. Absorption spectra of $\mathbf{[Pt(L)Cl_2]}$ upon addition of ct-DNA. Complex concentration = 25 μM; [DNA] = 0–100 μM (DNA concentration determined at λ = 260 nm, with ε = 6600 M^{-1} cm^{-1}). The MLCT band at λ = 257-259 nm was used to determine K_b (insert). The blue arrow shows (i) the decrease in absorption intensity with the increase of [ct-DNA] and (ii) the slight red shift of the absorption upon addition of ct-DNA.

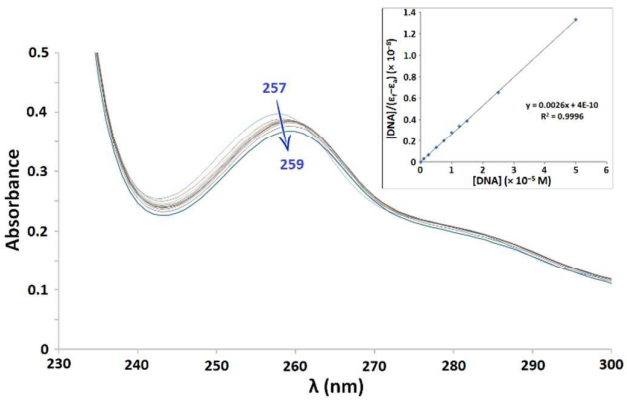

Figure 4. Emission spectra of the EB-DNA complex ([c] = 25 μM), λ_{exc} = 514 nm, λ_{em} = 610 nm, upon addition of increasing amounts of $\mathbf{[Cu(L)Cl_2]_2}$ (0–200 μM). The blue arrow shows the diminution in emission intensity with the increase of [complex]. Insert: I_0/I *vs.* [complex] plot for the titration of EB-DNA with $\mathbf{[Cu(L)Cl_2]_2}$; experimental data point and linear fitting of the data.

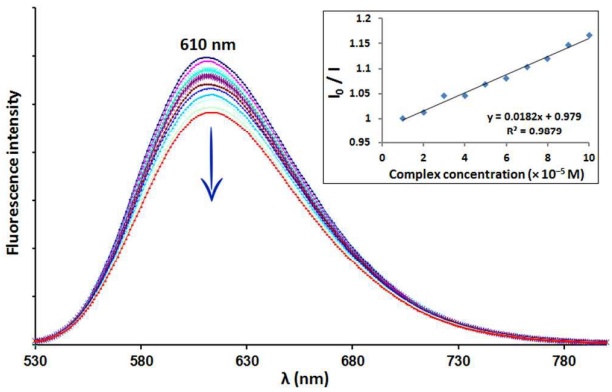

Figure 5. Plot of I_0/I *vs.* [complex] for the titration of EB-DNA with $\mathbf{[Pt(L)Cl_2]}$ at λ_{exc} = 514 nm and λ_{em} = 610 nm; experimental data point and fitting of the data. [complex] = 0–150 μM; [ct-DNA] = 25 μM and [EB] = 125 μM. Insert: linear fitting of the data for [complex] = 0–15 μM.

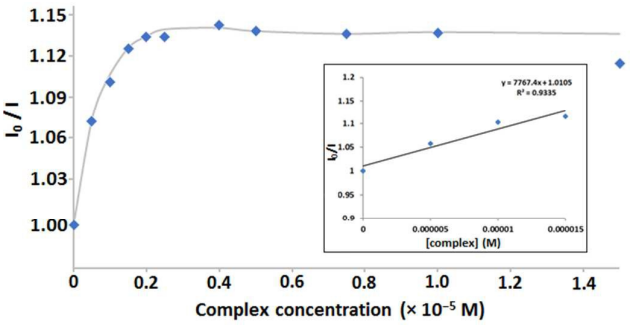

View Article Online
DOI: 10.1039/C7DT04604A

Figure 6. Agarose gel electrophoresis images of pBR322 plasmid DNA incubated for 24 h at 37 °C with increasing concentrations of a) **$[Cu(L)Cl_2]_2$** and b) **$[Pt(L)Cl_2]$**.

a) Lane 1: pure plasmid DNA; lanes 2–8: without reducing agent – lane 2: [complex] = 5 μM, lane 3: [complex] = 10 μM, lane 4: [complex] = 20 μM, lane 5: [complex] = 40 μM, lane 6: [complex] = 60 μM, lane 7: [complex] = 80 μM, lane 8, [complex] = 100 μM – lane 9: [Sigman's reagent] = 40 μM; lane 10: [Sigman's reagent] = 40 μM + [ascorbic acid] = 1 mM; lane 11: pure plasmid DNA; lane 12: DNA + [ascorbic acid] = 1 mM; lanes 13-19: with reducing agent ([ascorbic acid] = 1 mM) – lane 13: [complex] = 5 μM, lane 14: [complex] = 10 μM, lane 15: [complex] = 20 μM, lane 16: [complex] = 40 μM, lane 17: [complex] = 60 μM, lane 18: [complex] = 80 μM, lane 19, [complex] = 100 μM.

b) Lane 1: pure plasmid DNA; lane 2: DNA + cisplatin (0.5 equiv.); lane 3: DNA + cisplatin (1.0 equiv.); lane 4: [complex] = 10 μM; lane 5: [complex] = 15 μM; lane 6: [complex] = 50 μM; lane 7: [complex] = 100 μM.